35th Annual International Conference of the IEEE EMBS
Osaka, Japan, 3 - 7 July, 2013

A Robust Hair Segmentation and Removal Approach for Clinical Images of Skin Lesions*

Adam Huang, Shun-Yuen Kwan, Wen-Yu Chang, Min-Yin Liu, Min-Hsiu Chi, and Gwo-Shing Chen

Abstract— **Artifacts such as hair are major obstacles to automatic segmentation of pigmented skin lesion images for computer-aided diagnosis systems. It is even more challenging to process clinical images taken by a regular digital camera, where the shadows of the skin texture may mimic hair-like curvilinear structures. In this study, we examined the popular DullRazor software with a dataset of 20 clinical images. The software, specifically designed for dermoscopic images, was unable to remove fine hairs or hairs in the shade. Alternatively, we proposed using conventional matched filters to enhance curvilinear structures. The more complicate hair intersection patterns, which were known to generate low matched filtering responses, were recovered by using region growing algorithms from nearby detected hair segments with linear discriminant analysis (LDA) based on a color similarity criterion. The preliminary results indicated the proposed method was able to remove more fine hairs and hairs in the shade, and lower false hair detection rate by 58% (from 0.438 to 0.183) as compared to the DullRazor's approach.**

I. Introduction

With emerging development of sophisticated computer-aided image analysis technologies, a remarkable interest has arisen for dermatologists to seek an objective second opinion from computer-aided diagnosis (CAD) software for assisting skin lesion malignancy diagnosis. In dermatology, however, the majority of CAD development so far has been mainly focused on melanoma or melanocytic skin cancer detection using dermoscopic images [1, 2]. The reason is that melanoma is the most dangerous form of skin cancer. It causes the majority (75%) of deaths related to skin cancer [3]. Since the incidence rates of melanoma in the Asian population are much lower than the Caucasian population [4], it drew our attention to develop a CAD system that is capable of classifying non-melanocytic skin cancers for the Asian population as well.

In one of our ongoing research projects, we collected clinical images of skin lesions that were recorded using regular digital cameras [5]. Clinical images, or called macroscopic images, are photographs that reproduce what a clinician sees with the naked eye. The rationale to use clinical images for CAD is that the superficial characteristics such as diminishing texture and pores (which are useful diagnostic patterns for certain cancers such as basal cell carcinoma (BCC)) are visible in clinical images but not under dermoscopy examinations. Another concern is that the effectiveness of dermoscopy for non-melanocytic lesions is still unknown. As BCCs are far more common in our hospital and digital cameras are easily accessible, a CAD system devoted to process the clinical images of other types of cancers such as BCCs could be more beneficial to our clinicians.

There are various imaging artifacts needed to be removed so that the skin lesions can be segmented more consistently by a CAD software system. Among artifact pre-processing methods, hair removal algorithms [6-8] stand out as one of the most studied subjects. This phenomenon is not surprising because human skin is covered by various types of hair which may be dark or light, thick or thin, dense or sparse. These diverse patterns make hair detection a rather complicated task as compared to blood vessel segmentation [9-11]. Although hairs maybe better physically shaved before lesions are photographed, the presence of hair or pores can help differentiate benign lesions from BCCs. Therefore, skin lesions prepared for clinical imaging are commonly not clean-shaven to keep the trace of hair for diagnosis purpose.

In this study, we first evaluated a popular hair removal software, DullRazor [6], on a set of 20 clinical images. We found that fine hairs and hairs in the shade were more difficult to detect by using DullRazor due to less consistent lighting conditions in clinical images. Second, multiscale matched filters [5, 9] for detecting retina vessels were revised and implemented to improve the detection of shaded and fine hairs for clinical images.

II. Materials and Methods

A. Data Acquisition

The clinical images of skin lesions were selected from a database from the Kaohsiung Medical University Hospital in Taiwan [5]. In this database, a suspicious region was photographed by using a Nikon D70 6.1 megapixel digital single-lens reflex (SLR) camera and sigma 18-50 mm F2.8 macro lens. Biopsy was performed and histopathology result was available for each lesion. From this database, a small testing dataset of 20 skin lesion images with visible, various hair and pigment patterns were selected to examine the performance of DullRazor software and the proposed hair detection algorithm.

*Resrach supported by the National Science Council of Republic of China (Taiwan) under Grants NSC 101-2221-E-008-021 and NSC 101-2911-I-008-001.

A. Huang is with the Research Center for Adaptive Data Analysis/Center for Dynamical Biomarkers and Translational Medicine/Graduate Institute of Biomedical Engineering, National Central University, Jhongli, Taiwan. (e-mail: adamhuan@ncu.edu.tw)

S.-Y. Kwan, M.-Y. Liu, M.-H. Chi are with the Institute of Systems Biology and Bioinformatics, National Central University, Jhongli Taiwan.

W.-Y. Chang is with E-Da Hospital, I-Shou University and the Graduate Institute of Medicine, Kaohsiung Medical University, Kaohsiung, Taiwan.

G.-S. Chen is with the Department of Dermatology, Kaohsiung Medical University Hospital, Kaohsiung, Taiwan.

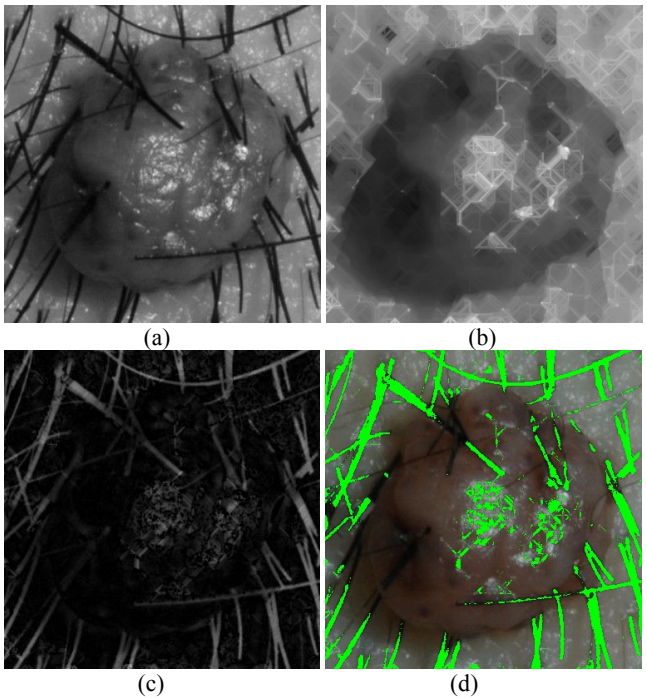

Figure 1. (a) Grayscale image of a skin lesion with hairs. (b) Closing image of the grayscale image in (a). (c) The difference between closing image (b) and the original grayscale image (a). (d) Hair mask (in green color) detected by thresholding on intensity values in image (c).

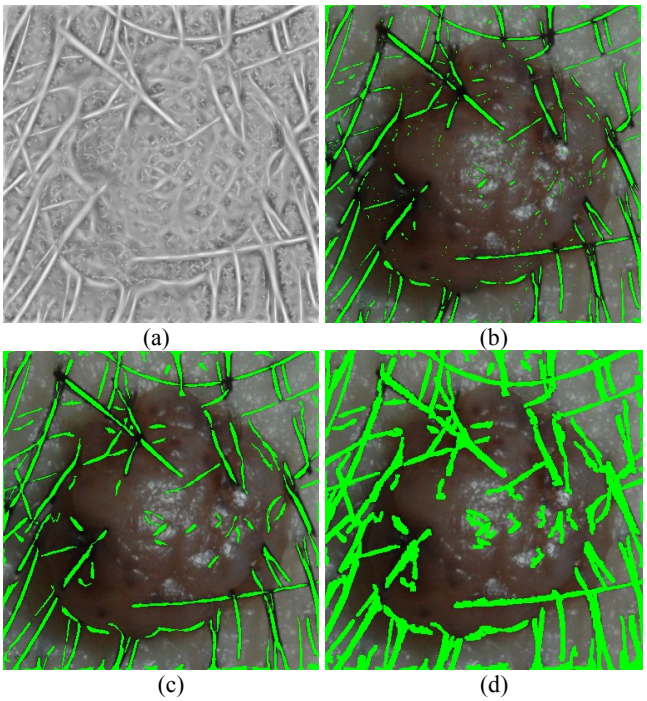

Figure 2. (a) Multiscale matched filtering responses for Fig 1(a). (b) Hair detection by using a single, higher threshold. (c) Hair detected using hysteresis thresholding with two values. (d) Region growing based on color similarity by LDA in the CIELab color space.

B. *DullRazor: Morphological Closing*

It is quite natural for us to first consider adopting available pre-processing methods that are originally developed for dermoscopic images. The DullRazor software was first introduced in 1997 [6] to digitally remove dark hairs from dermoscopic images, and is now widely used in the field of dermatology [8]. The key technique that DullRazor uses to locate thick dark hair pixels is a generalized grayscale morphological closing operation with a group of directional structure elements for specific curvilinear properties. The grayscale closing operation *smoothes* out the low intensity values at the thick dark hair pixels according to the structure element used to probe the image. From a geometrical point of view, the dark hairs appear like troughs in a terrain model. The closing operation basically elevates the troughs according to the span of the directional structure element. In [6], three directional structure elements at 0 degrees (horizontal), 45 degrees (diagonal), and 90 degrees (vertical) are used to smooth out all the dark hairs. In our implementation for illustrating Fig 1, we included a fourth direction: 135 degrees (anti-diagonal). The maximum values among 4 directions were collected as the final result.

Fig 1 delineates an example of DullRazor's approach. Fig 1(a) illustrates the grayscale image of an input skin lesion and Fig 1(b) its resultant closing image using 4 directional structure elements. Fig 1(c) illustrates the difference between Figs 1(a), the original image, and 1(b), the closing image. In Fig 1(c), one can easily observe that a higher difference value is more likely to correspond the pixel to a dark hair. However, skin texture which resembles dark hairs also generates high difference pixel values at the central region of Fig 1(c).

Another drawback by using a closing operation is that fine hairs and thick dark hairs in the shade or within darker background have lower difference values. Fig 1(d) shows a hair mask (in green color) by thresholding on Fig 1(c). It demonstrates that DullRazor approach cannot detect fine and shaded hairs in clinical images.

In order to increase the detection success rate, we need a more sensitive method to be able to detect thin and shaded hairs more consistently and robustly. Multiscale matched filters which are able to enhance blood vessels of different diameters is a good candidate method which is delineated as follows

C. *Matched Filtering*

2D matched filters are shape-specified pixel patterns which convolve with a grayscale image to find similar patterns within the image. Matched filters have been used to detect blood vessels for clinical skin images [5]. Here we test its applicability to hair detection for similar clinical images.

Multiscale curvilinear matched filtering. Similar to retina image processing, the color image is first transformed into a grayscale image. Because 2D lines in a grayscale image appear like ridges or trenches in a terrain model, a typical matched filter, F_M, is a pixel value pattern resembling a ridge shape with a Gaussian-like profile:

$$F_M(x, y; \sigma_f) = \exp\left(- \frac{[(P - P_0) \cdot \mathbf{v}]^2}{2\sigma_f^2} \right) \qquad (1)$$

where P is any point (x, y), P_0 is the center (x_0, y_0) of the filter, and **v** is a unit vector perpendicular to the line tangent direction. F_M is commonly defined in a square matrix of $(x_0 \pm 3\sigma_f, y_0 \pm 3\sigma_f)$.

In order to convolve with ridge-shaped F_M, defined in Eq (1), the grayscale image needs to be inverted so that dark hairs can be enhanced correctly. The neighborhood $I(x \pm 3\sigma_f, y \pm 3\sigma_f)$ of a tested pixel (x, y) also needs to be normalized to pixel values ranging from 0 to 1 before convolving with Eq (1). Let Z denote the filter response at a point (x, y) by matched filter F_M defined with a standard deviation σ_f

$$Z(x, y; \sigma_f) = \frac{\left(\Sigma_i \Sigma_j I(x+i, y+j) \times F_M(x+i, y+j)\right)^2}{\left(\Sigma_i \Sigma_j \left(I(x+i, y+j)\right)^2\right)\left(\Sigma_i \Sigma_j \left(F_M(x+i, y+j)\right)^2\right)} \quad (2)$$

where i, j are integers between $-3\sigma_f$ and $+3\sigma_f$.

The multiscale curvilinear matched filtering repeats the computation (2) using a set of 4 discrete standard deviation values $\sigma_f \in \{1, \sqrt{2}, 2, 2\sqrt{2}\}$ and a set of 12 directions for **v** in (1) as suggested in [9]. The maximum response Z is collected. The result of line-matched-filtering enhanced image for Fig 1(a) is shown in Fig 2(a).

Thresholding with hysteresis. Hairs in the line enhanced images are extracted by thresholding with hysteresis. John Canny's two-level thresholding with hysteresis is an effective edge detection algorithm which can trace the curve of an edge with faint sections [12]. It works the same way for matched filtering curvilinear structures. The algorithm assumes that important linear structures are more likely to have high enhanced responses. Therefore, a high threshold can be used to identify the major hair sections. The detected hairs (in green color) shown in Fig 2(b) is the resultant image using a high threshold of 0.75 on the enhanced image shown in Fig 2(a). While partial segments of hair may be situated at some more noisy background, these hair segments may be enhanced but with a lower filtering response value. Therefore, hysteresis thresholding uses a secondary threshold, which is lower, to extend the hair segmentation extracted by the high threshold. Fig 2(c) shows the extended hair segmentation (in green color) by a low threshold of 0.65. Small detected line segments are considered as noise caused false detections and they are removed in Fig 2(c).

D. Recovering Hair Intersections

The intersections of ridges are known to generate low filtering responses due to high shape difference from a pure ridge structure. Fig 2(c) shows that the majority of hair intersections are still missing even with a lower threshold. To improve our hair segmentation algorithm, we proposed using machine learning techniques such as linear discriminant analysis (LDA) [13] to recover missing hair intersections from partial information of hair color pixel values discovered in Fig 2(c). Generally speaking, LDA uses two measures to separate classes of data samples: 1) within-class scatter matrix

$$S_w = \sum_{j=1}^{c} \sum_{i=1}^{N_j} (\mathbf{x}_i^j - \mu_j)(\mathbf{x}_i^j - \mu_j)^T \quad (3)$$

and 2) between-class scatter measure matrix

$$S_b = \sum_{j=1}^{c} (\mu_j - \mu)(\mu_j - \mu)^T \quad (4)$$

where $\mathbf{x}_i^j$ is the i-th sample of class j, μ_j is the mean of class j, c is the number of classes, and N_j the number of samples in class j, μ is the mean of all classes.

For discriminating classes, the goal is to maximize the between-class measure while minimizing the within-class measure. One way to do this is to maximize the ratio $\det|S_b| / \det|S_w|$. It has been proven [14] that if S_w is a nonsingular matrix then this ratio is maximized when the data is projected onto a new space defined by the eigenvectors of $S_w^{-1} S_b$. Since we only employed sample color information from both hair and non-hair pixels defined in the CIELab color space with 3 variables of L, a, and b, we were able to efficiently build linear classifiers locally for every pixel under consideration. By using region growing algorithms and local LDA results based on the pixel color information, hair intersections can be recovered very effectively and accurately. Fig 2(d) shows the much improved hair detection results as compared to Fig 1(d).

III. RESULTS

Figs 3 and 4 illustrate two hair removal examples to compare DullRazor and the proposed line-filtering algorithm. Fig 3 is a lesion with some thick dark hairs located in shade and Fig 4 is a lesion with both thick and fine hairs. Figs 3(b) and 4(b) show that closing operations fail to remove hairs in the shade and fine hairs respectively. Figs 3(c) and 4(c) demonstrate that our proposed line-filtering approach is able to detect all kinds of hair, thin or thick, situated in a bright or shaded background. Finally, Figs 3(d) and 4(d) show that hairs can be removed more robustly by using the proposed approach as compared to Figs 3(b) and 4(b). Please note that Figs 3(b) and 4(b) were processed by the DullRazor software [6] while hair pixels in Figs 3(d) and 4(d) were removed by using median filtering from non-hair neighbors. Fig 5 shows that the proposed method can lower false hair detection rate by 58% (from 0.438 to 0.183) at the true detection rate of 0.81.

IV. CONCLUSION

We have presented an improved hair segmentation algorithm for clinical images of skin lesions. We found that matched filtering can improve the detection of thin hairs and hairs in the shade. We also demonstrated that missing hair intersections can be recovered effectively by applying region growing algorithms with color similarity criteria.

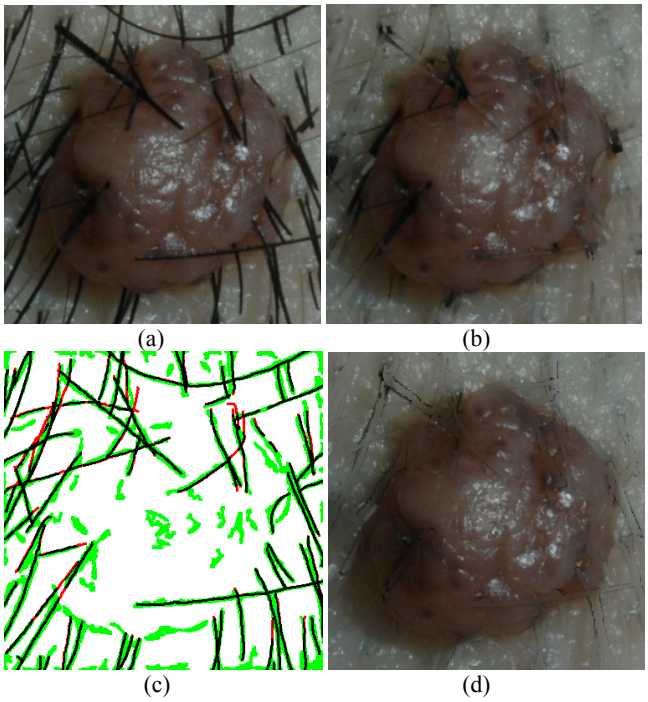

Figure 3. (a) Original clinical image of thick dark hairs in the shade. (b) Hair removal by using DullRazor. (c) Hair segmentation: green pixels are detected by the proposed method only, red by manual marking only, and black by both manual marking and the proposed method. (d) Hair removal by using the proposed method.

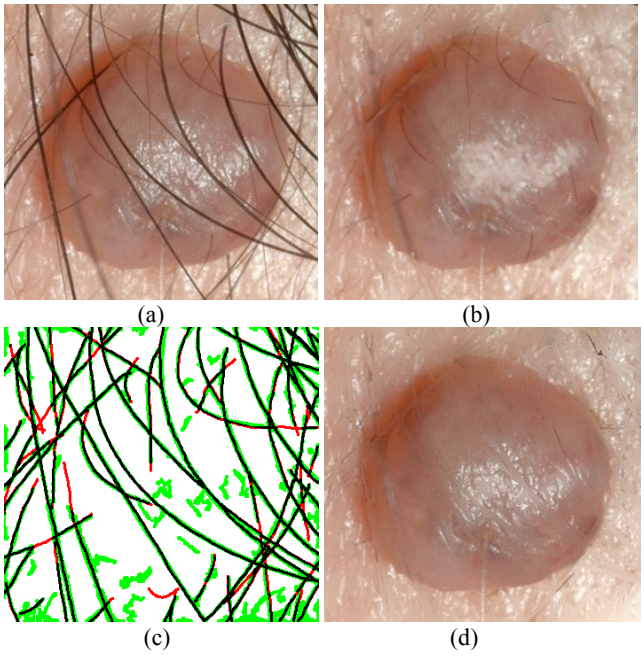

Figure 4. (a) Another example lesion with both thick and fine hairs. (b) Hair removal by using DullRazor. (c) Hair segmentation: green pixels are detected by the proposed method only, red by manual marking only, and black by both manual marking and the proposed method. (d) Hair removal by using the proposed method.

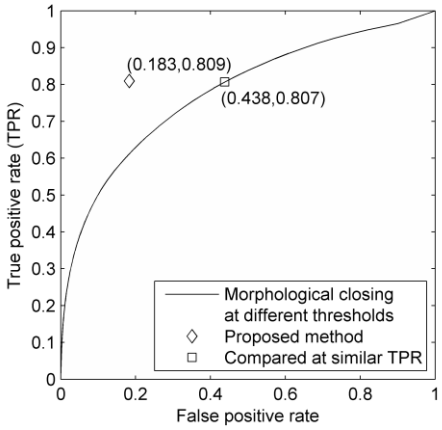

Figure 5. True and false positive rates of detecting hair pixels computed from 20 clinical images and manually marked hair masks.

REFERENCES

[1] K. Hoffmann, T. Gambichler, A. Rick et al, "Diagnostic and neural analysis of skin cancer (DANAOS), A multicentre study for collection and computer-aided analysis of data from pigmented skin lesions using digital dermoscopy," *British Journal of Dermatology*, vol. 149, pp. 801-809, 2003.

[2] R. LeAnder, P. Chindam, M. Das et al, "Differentiation of melanoma from benign mimics using the relative color method," *Skin Research and Technology*, vol. 16, pp. 297-304, 2010.

[3] A.F. Jerant, J.T. Johnson, C.D. Sheridan, T.J. Caffrey, "Early detection and treatment of skin cancer," *American Family Physician*, vol. 62, pp. 357-368, 2000.

[4] J. Sng, D. Koh, W.C. Siong, T.B. Choo, "Skin cancer among Asians living in Singapore from 1968 to 2006," *Journal of the American Academy of Dermatology*, vol. 61, pp. 426-432, 2009.

[5] A. Huang, W.Y. Chang, H.Y. Liu, and G.S. Chen, "Capillary detection for clinical images of basal cell carcinoma," in *Proc. ISBI*, pp. 306-309, 2012.

[6] T. Lee, V. Ng, R. Gallagher, A. Coldman, D. McLean, "Dullrazor: a software approach to hair removal from images," *Computers in Biology and medicine*, vol. 27, pp. 533-543, 1997. Software Available at http://www.dermweb.com/dull_razor/

[7] A. Abbas, M.E. Celebi, I.F. Garcia, "Hair removal methods: a comparative study for dermoscopy images," *Biomedical Signal Processing and Control*, vol. 6, pp. 395-404, 2011.

[8] K. Korotkov, R. Garcia, "Computerized analysis of pigmented skin lesions: a review," *Artificial Intelligence in Medicine*, in press.

[9] S. Chaudhuri, S. Chatterjee, N. Katz, M. Nelson, and M. Goldbaum, "Detecion of blood vessels in retinal images using two-dimensional matched filters," *IEEE Transactions on Medical Imaging*, vol. 8, pp. 263-269, 1989.

[10] A. Hoover, V. Kouznetsova, and M. Goldbaum, "Locating blood vessels in retinal images by piecewise threshold probing of a matched filter response," *IEEE Transactions on Medical Imaging*, vol. 19, pp. 203-210, 2000.

[11] J. Staal, M.D. Abramoff, M. Niemeijer, M.A. Viergever, and B. can Ginneken, "Ridge-based vessel segmentation in color images of the retina," *IEEE Transactions on Medical Imaging*, vol. 23, pp. 501-509, 2004.

[12] J. Canny, "A computational approach to edge detection," *IEEE Transactions on Pattern Analysis and Machine Intelligence*, vol. 8, pp. 679-698, 1986.

[13] A.M. Martinez, A.C. Kak, "PCA versus LDA," *IEEE Transactions on Pattern Analysis and Machine Intelligence*, vol. 23, pp. 228-233, February 2001.

[14] R.A. Fisher, "The statistical utilization of multiple measurements," *Annals of Eugenics*, vol. 8, pp. 376-386, 1938.